



OPEN

U(VI) removal from diluted aqueous systems by sorption–flotation

Carolina Constantin¹, Ioana-Carmen Popescu^{2✉}, Ovidiu Oprea¹ & Ligia Stoica¹

The legacies of past uranium mining and milling activities for nuclear fuel fabrication continue to be a cause of concern and require assessment and remedial action for researchers worldwide. The discharge of uranium contaminated water into the environment is a matter of regulation (World Health Organization, WHO—15 µg/L, Romanian Legislation, RO—21 µg/L), environment and health. Therefore, various removal technologies of U(VI) from diluted aqueous solutions include chemical precipitation, ion exchange, adsorption, immobilization on zero-valent iron nanoparticles, etc. have been extensively applied. Our previous research has studied the removal of U(VI) from diluted aqueous systems such as mine waters using Fe⁰-based nanomaterials synthesized in the laboratory (NMS) (Crane et al. in *Water Res* 45:2391–2942, 2011). The carbonate rich aqueous system was treated with NMS to remove U(VI). It was observed that after half an hour of reacting time only about 50% was removed due to its high tendency to form stable soluble carbonated complexes. Considering that, the present article aims to investigate the Sorption/Flotation technique, by using a sorbent generated in situ Fe₂O₃·nH₂O and sodium oleate surfactant to remove U(VI) from diluted aqueous systems and to update the knowledge on the mechanism of process. In order to determine the removal efficiency of U(VI), the influencing factors were studied: pH, sorbent dose, surfactant concentration, contact time, stirring rate, the U(VI) concentration, air pressure in pressurized water recipient, and the effect of some accompanying heavy metals ions (Cu(II), Cr(VI), and Mo(VI)). The removal efficiency (%R) was monitored and its maximum values allowed to establish the optimal separation parameters (the established process parameters), which were validated on real mine water samples (MW). High U(VI) removal efficiencies %R > 98% were obtained. The Sorption/ Flotation technique was applied to remove U(VI) from two types of real mine water samples, namely “simple” and “pre-treated with NMS”, respectively. For the mine water samples pre-treated with NMS, it worked in two variants: with and without pH correction. For pH range = 7.5–9.5, molar ratios [U(VI)] : [Fe(III)] = 1 : 75, [U(VI)] : [NaOL] = 1 : 1 × 10⁻², contact time 30 min., stirring speed 250 RPM, initial concentration of U(VI) 10 mg·L⁻¹, air pressure in pressurized water recipient $p = 4 \times 10^5 \text{ N}\cdot\text{m}^{-2}$ is obtained %R > 98%. It has been found that Sorption / Flotation can function with good %R values as a stand-alone operation or in tandem with NMS pre-treatment of mine water and pH adjustment proved to be highly efficiency ($C_{\text{U(VI)}} < 1 \cdot 10^{-3} \text{ mg}\cdot\text{L}^{-1}$).

Radioactive pollution of the environment caused by uranium ores hydrometallurgical processing, in addition to the cross-contamination generated by other heavy metals used in this industry, is still a challenge for scientists, and a major threat to human health worldwide^{2–4}. Mine water generated by the weather events is an important radioactive pollutant and mobilizes significant amounts of U(VI), in addition to other accompanying heavy metals such as Cu (II), Cr (III + VI), and Mo (VI), and consequently, needs highly efficient remediation technologies^{3,5}. Unfortunately, the developed remediation technologies such as complexing processes⁶, co-precipitation^{7–10}, redox reactions⁹, ion exchange^{11,12}, solvent extraction^{13,14}, adsorption on different materials^{15–19}, bioremediation^{20,21} and immobilization on nanomaterials^{5,18,22–26} presents specific advantages and disadvantages. One example for specific advantage is the develop of new sorbents with changed properties that offer a multitude of improved applications, including selectivity. In case of removal of uranium from aqueous solution some research can be noticed for this purpose. Chitosan cross-linked using glutaraldehyde in the presence of magnetite. The resin was chemically modified through the reaction with tetraethylenpentamine (TEPA) to produce amine

¹Department of Inorganic Chemistry, Physical-Chemistry and Electrochemistry, Faculty of Applied Chemistry and Materials Science, University “POLITEHNICA” of Bucharest, 313 Splaiul Independentei, 060042 Bucharest 6, Romania. ²Research and Development National Institute for Metals and Radioactive Resources, INCDMRR-ICPMRR, Laboratory of Environment Protection Technics and Technologies, 70 Blvd. Carol I, 020917 Bucharest 2, Romania. ✉email: janepopescu@gmail.com

bearing chitosan. This resin showed a higher affinity towards the uptake of UO_2^{2+} ions from aqueous medium²⁷. Schiff's base chitosan composite with magnetic properties. This composition showed high affinity and fast kinetic for the sorption of UO_2^{2+} ions²⁸. Magnetic chitosan nanoparticles functionalised by grafting diethylenetriamine (DETA) and dithizone for improving U(VI) sorption at pH around 5²⁹. The phosphorylation of guar gums combined with chitosan preparing an efficient sorbent for the removal of U(VI) from slightly acid solutions. In addition if it is done phosphorylation of guar gums/magnetite/chitosan nanocomposites has antibacterial effects against both Gram+ and Gram- bacteria³⁰. Another interesting new sorbent for U(VI) are silica beads functionalized with urea or thiourea-based polymers³¹. Examples for disadvantages are the chemical methods, ion exchange, and solvent extraction. There are highly efficiency in treating effluents that contain large amounts of pollutants, but are prohibitive in remedying diluted aqueous systems (10^{-3} – 10^{-6} M solutions).

Flotation is one of the absorptive bubble separation techniques, which involves the removal of surface inactive ions from homogeneous and heterogeneous aqueous systems by the introduction of a surfactant to become surface-active ions and subsequent passage of gas micro disperse bubbles through the solution in a foam separation column. The surface-active ions, which are absorbed on the surfaces of the rising bubbles, can be carried upward to the top of the foam separation column, and thus removed from the aqueous system as condensed foam (sublate).

In the separation process the properties of participant phases are important: superficial interface properties of liquid phase; high hydrophobia and low density for species in foam concentrated; homogeneous dimension of gas bubbles, which provides the mass transfer liquid-foam; the optimum gas flow for the bubble-particles aggregation in foam.

The different technological variants such as ion flotation^{4,32–35}, precipitate flotation³⁶, sorption–flotation^{12,35,37–40}, colloidal adsorbing flotation⁴¹, electro-flotation⁴², flotoextraction^{43,44}, have proved their highly decontamination efficiency of a wide variety of diluted aqueous systems^{45–52}.

The main advantages are high selectivity, adaptability, high removal efficiency, possibility of being applied for the removal of ionic, molecular, colloidal, and micro-dispersed species of inorganic or organic nature^{35,48–52}. However, some of them have disadvantages, namely electro-flotation, which consumes energy, and the flotation with dispersed gas, which provides non-homogenous bubbles and requires high quality and resistant porous material. Among the bubble generation techniques, the Dissolved Air Flotation (DAF) technique is preferred because it provides small homogeneous bubbles in situ.

DAF application involves two variants: (a) direct pressurization by introducing the airflow into the water sample conditioned with reagents subjected to flotation; (b) dilution with recirculated water under pressure of the sample conditioned with reagents, before flotation. Industrial is the last option because it is cost-effective and works in small, compact, and relatively simple installations. Rapidity (flotation contact time is less than 5 min.), versatility (removal of organic substances and heavy metals such as copper, chromium and molybdenum), simplicity of installation, are other advantages that recommend this method of separation.

The mobility of U(VI) is largely dependent on changes in pH, variation of redox potential in the environment, and the presence of other neutral and/or ionic species, such as humic acids, sulfate, phosphate, and carbonate ions, which interact with the uranyl ions, and turns them into highly soluble complexes. For example, carbonate generates highly stable uranyl-carbonate complexes and plays a key role in its biogeochemistry and bioavailability⁵³.

Considering the complex chemistry of uranium-contaminated mine waters, in addition to environmental pollution caused by other industries using toxic heavy metals such as Cu (II), Cr (VI), and Mo (VI), this study aims to investigate the removal of U(VI) by Sorption / Precipitate flotation from mono- and multi-contaminated aqueous systems as natural analogues, and, respectively, real mine water samples, in order to update the acquired knowledge on the process mechanism.

The sorbent used in this study is generated in situ consists of $\text{Fe}_2\text{O}_3 \times n \text{H}_2\text{O}$ and was selected considering iron's physicochemical properties and high separation efficiency of a wide variety of contaminants, including U(VI) and the accompanying heavy metals^{5,23,24,54}. This choice was made to obtain the advantages offered by: (i) the circulation of a small volume of reagent with Fe(III) to generate the adsorbent support; (ii) the reduction of the costs of adsorbent support obtaining; (iii) ensuring the optimal contact with U(VI) through its loose and flaky structure; (iv) the reduction of the reaction time and the volume of waste generated. Although iron hydroxide is not unique, it is an environmentally friendly and low cost alternative to synthesized sorbents.

In order to increase the hydrophobicity of the sorbent loaded with U(VI), a collector (surfactant) was introduced into the system, which in this case is sodium oleate (NaOL), $\text{C}_{18}\text{H}_{33}\text{O}_2\text{Na}$. It has been preferred over others because it is a common and inexpensive reagent due to its low toxicity, accessibility, high availability, and proven safety in its food uses as a binder, emulsifier, anticaking agent, and indirect additive⁵⁵. The long C-chain of sodium oleate explains the high hydrophobicity and surface-active (surfactant) properties of sodium oleate^{48–52}.

The research presented in this paper is justified by the practical scientific interest shown above^{4,12,32–35,37–39}.

Previous research¹ on the removal of U(VI) on Fe^0 -based nanomaterials synthesized in the laboratory (NMS) have proved their efficiency in U(VI) removal from carbonate-rich mine water in about one hour, but after more than 24 h of reaction time a desorption process due to the soluble appearance of uranyl-carbonate complexes⁵. Thus, the combined NMS—Sorption/Flotation tandem technology is becoming a promising treatment alternative. Therefore, the novelty of this paper compared to previous research is the proposal of a new remedial technology that uses the reactivity of iron-based nanomaterials and separation efficiency of DAF technique.

Materials and method

Reagents. All the reagents were MERCK analytical grade. All solutions were prepared using Mili-Q purified water (resistivity > 18.2 MΩ cm).

- $\text{Na}_4[\text{UO}_2(\text{CO}_3)_3]$, stock solution ($1 \text{ g}\cdot\text{L}^{-1}$ U(VI)), and work solution ($10 \text{ mg}\cdot\text{L}^{-1}$) were prepared using uranyl acetate ($\text{UO}_2(\text{CH}_3\text{COO})_2\cdot\text{H}_2\text{O}$) and anhydrous sodium carbonate (Na_2CO_3);
- $\text{Cu}(\text{NO}_3)_2$, $\text{MoO}_3\cdot\text{H}_2\text{O}$, and K_2CrO_4 , work solutions ($10 \text{ mg}\cdot\text{L}^{-1}$) of Cu(II), Cr(VI), and Mo(VI);
- NaOH and HCl, pH adjustment solutions (0.01 M and 0.1 M);
- FeCl_3 , solutions (0.01 M and 0.1 M) for sorbent in situ generated;
- NaOL solutions: 0.25 M , $0.25 \times 10^{-3} \text{ M}$ and $0.025 \times 10^{-3} \text{ M}$.
- NMS (Fe^0 -based nanomaterials) synthesized in the laboratory¹

Equipment.

- Heidolph Vibramax 100 stirrer, with variable speed.
- 290A ORION pH-meter;
- UNICAM PAY SP9 atomic absorption spectrophotometer for Cu (II), Cr (VI), and Fe (III) determination;
- CINTRA 404 UV-VIS spectrophotometer for U(VI) and Mo (VI) determination.
- UHPLC PLATINblue for NaOL determination
- FT-NIR spectrophotometer MB3600-AAA for IR spectra.
- Netzsch analyzer TG 449 C STA Jupiter for solid samples thermal analysis.

Experimental method. *Sorption/flotation experiments with sorbent generated in situ.* The experiments were performed in batch mode. The U(VI) sample (200 mL) was contacted with Fe (III) solution mixed with NaOH 0.1 M at various molar ratios [U(VI)]: [Fe (III)] stirred continuously for a previously set time of 30 min⁵⁶. After adjusting the pH, the sample was contacted with the surfactant, (NaOL) in various molar ratios [NaOL]: [U(VI)] and transferred to the flotation cell, which is coupled to a pressured water recipient. The recipient is filled with water saturated with air at a pressure of $5 \times 10^5 \text{ N}\cdot\text{m}^{-2}$. An aliquot of water under pressure (dilution ratio $V_{\text{sample}}:V_{\text{water}} = 3 : 1$) was introduced into the base of the flotation cell and uniform-sized microbubbles were generated. Thus, they adhered to the surface of the formed solid (sorbent generated in situ and U(VI) loaded on its surface) and it rises to the top of flotation cell. The flotation time was 5 min until all foam was separated at the top. The residual concentration of U(VI), Fe (III), and NaOL was analyzed. All experiments were triplicated.

The study of influencing factors (pH, molar ratio, metallic ion concentrations, necessary air, etc.) by $\%R = f(\text{property})_{\text{max}}$ established the optimum conditions for U(VI) separation.

The removal efficiency was calculated according to the equation:

$$\%R = [(C_i - C_f)/C_i] \times 100, \quad (1)$$

where,

- C_i is the initial concentration of metallic ions ($\text{mg}\cdot\text{L}^{-1}$);
- C_f is the final concentration of metallic ions ($\text{mg}\cdot\text{L}^{-1}$).

The adsorption process of U(VI) under working conditions is characterized by an isothermal dynamics and the kinetic models, respectively. The obtained results⁵⁶ suggest that the process is mixed and involves both physical and chemical interactions between U(VI) and Fe(III) aqueous species (co-precipitation). Based on the correlation coefficients (R²), the sorption equilibrium data fitted to the isotherm models in the following order: Langmuir (0.9808) > Temkin (0.8715) > Freundlich (0.8344). The close values of KF, Q_{exp} and Q_{calc} suggest that the process involve chemisorption in good agreement with the fact that it has followed the pseudo-second order kinetics as confirmed by other studies^{57,58}.

Optimal parameters' validation experiments. Two types of mine water samples (MW), namely "simple" and "pre-treated with NMS" respectively ($V_{\text{sample}} = 400 \text{ mL}$, pH range = 7.5–9.5, $m_{\text{NMS}} = 0.1 \text{ g}$, $\tau_{\text{contact}} = 30 \text{ min}$, stirring rate 250 RPM) were subjected to previously studied Sorption/Flotation process. Mine water samples (MW1–3) were collected from a former uranium mining site situated in the Banat region.

Regarding the "pre-treatment with NMS" samples, it is mentioned that the nanomaterial used has the following characteristics¹:

- the surface area (by BET analysis) was $14.8 \text{ m}^2/\text{g}$ for over 80% of the studied nanoparticles;
- particle size distribution (by TEM analysis) in the range 0–50 nm;
- XRD analysis of crystallinity revealed disordered / amorphous structure;
- XPS analysis of chemical composition of the surface led to % Fe = 30.5, % O = 32.1, % C = 14.5 and % B = 22.9;
- oxide thickness (by XPS analysis) was 3–4 nm;
- surface chemistry ($\text{Fe}^0 / \text{Fe}^{2+} = 0.02$ and $\text{Fe}^{2+} / \text{Fe}^{3+} = 0.38$)¹;

Results and discussions

Influencing factors. *Flotation pH.* The pH is extremely important because it determines the charge, the structure, and the concentration of U(VI) species in dilute aqueous systems (Fig. 1). The U(VI) species were calculated using Phreeqc Interactive 3.2.2 software and lnl.dat database considering only the simple aqueous solution of $\text{Na}_4[\text{UO}_2(\text{CO}_3)_3]$ containing 0.042 mM U(VI) ($10 \text{ mg}\cdot\text{L}^{-1}$ U(VI)), respectively (main concentration

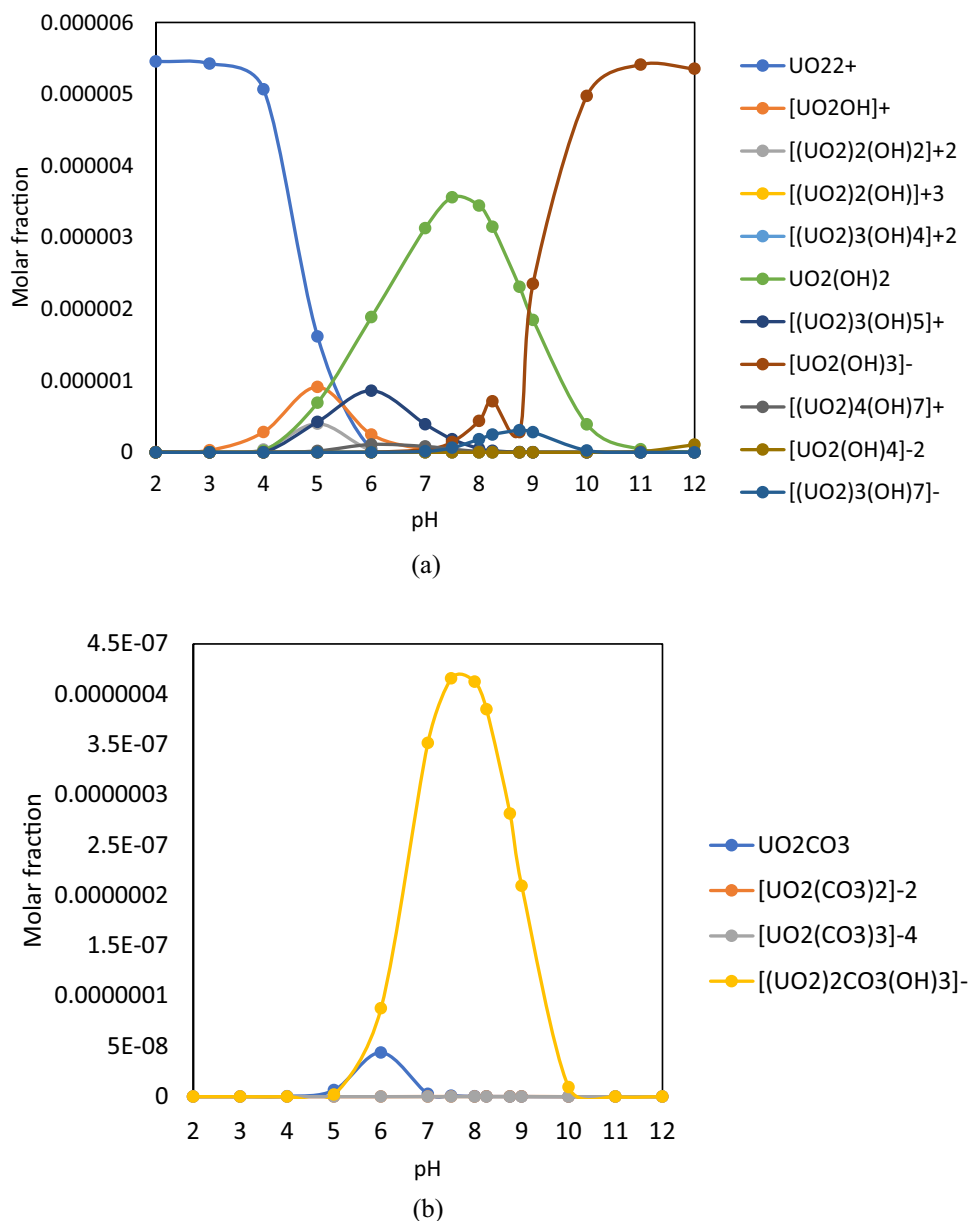


Figure 1. U(VI) species in the mixture U(VI) + Fe(III) calculated by Phreeqc Interactive 3.2.2 software and llnl.dat database. (a) hydroxide-complexes; (b)—carbonate-complexes.

of experimental samples). The pH ranged from 2 to 12 to cover all the types of natural waters, such as highly acidic ones from acid mining drainage and those from the uranium mining industry. The ionic strength was determined by the software.

Species calculations were performed taking into account the simple aqueous system containing only the simple chemical substance without any addition of salts to ensure a constant ionic strength. Ionic strength was calculated by the software. The sum of molar fractions was 1, considering all the species involved. Species with very small molar fractions were not displayed.

The curves obtained for $[\text{U(VI)}] = 0.042 \text{ mM}$ are in agreement with literature⁵⁹. According to the calculated data displayed in Fig. 1, the probable U(VI) species occurring in the pH range 7.0–9.5 are: (a) hydroxide complexes— $\text{UO}_2(\text{OH})_2$, $[\text{UO}_2(\text{OH})_3]^-$, $[(\text{UO}_2)_3(\text{OH})_7]^-$, and carbonate complexes— UO_2CO_3 , $[\text{UO}_2(\text{CO}_3)_2]^{2-}$, $[\text{UO}_2(\text{CO}_3)_3]^{4-}$ and $[(\text{UO}_2)_2\text{CO}_3(\text{OH})_3]^-$ in agreement with literature^{53,59}. The U(VI) hydroxide—and carbonate species were separately plotted, due to the different fraction ratios.

Figure 2 showed the sorbent Fe(III) species calculated by Phreeqc Interactive 3.2.2 software and llnl.dat database.

It is observed from Fig. 2 that $\text{Fe}_2\text{O}_3 \cdot n\text{H}_2\text{O}$ is formed in the pH range between 7.0–9.0, identical to that of $[(\text{UO}_2)_2\text{CO}_3(\text{OH})_3]^-$ and $\text{UO}_2(\text{OH})_2$. Therefore, as a result, there is a competition between these species.

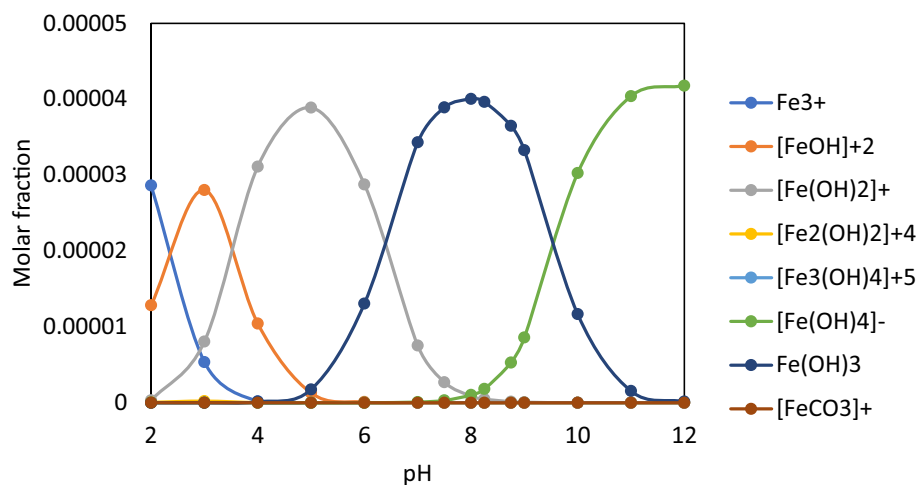


Figure 2. Fe (III) aqueous species in the mixture U(VI) + Fe(III) calculated by Phreeqc Interactive 3.1.1-8288 software using llanl.dat database.

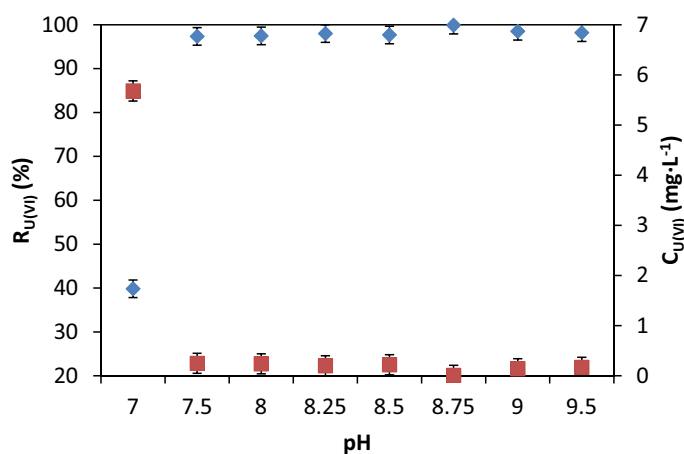


Figure 3. $\%R_{U(VI)}$ and $C_{U(VI)} = f(\text{pH})$, $V_{\text{sample}} = 200 \text{ mL}$, stirring rate 250 RPM, $[U(VI)]:[Fe(III)]:[NaOL] = 1:100:1$, contact time 30 min, $p = 4 \times 10^5 \text{ N}\cdot\text{m}^{-2}$, dilution ratio $V_{\text{sample}}:V_{\text{water}} = 3:1$

Their formation respects the ascending order of solubility product (K_{sp}) $K_{\text{sp, Fe(OH)}_3} = 4 \cdot 10^{-38} < K_{\text{sp, UO}_2(\text{OH})_2} = 1.1 \cdot 10^{-22} < K_{\text{sp, UO}_2\text{CO}_3} = 1.8 \cdot 10^{-12} < K_{\text{sp, FeCO}_3} = 10^{-10.560,61}$.

The influence of pH on removal efficiency has been studied on sorption / precipitate flotation by the function $\%R = f(\text{pH})$ (Fig. 3).

The U(VI) samples (200 mL) of $10 \text{ mg}\cdot\text{L}^{-1}$ U(VI) were contacted with Fe (III) solution at molar ratio $[U(VI)]:[Fe(III)] = 1:100$, which was determined by preliminary tests⁶² under constant stirring (250 RPM) for 30 min to generate the sorbent in situ ($\text{Fe}_2\text{O}_3 \cdot n\text{H}_2\text{O}$). The pH adjustment was performed in the pH range 7.0–9.5 corresponding to the maximum sorbent amount (Fig. 4). After adjusting the pH, the sample was contacted with the surfactant (NaOL) at the molar ratio $[\text{NaOL}]:[U(VI)] = 1:1$ ^{51,63}, transferred to the flotation cell and diluted in a dilution ratio $V_{\text{sample}}:V_{\text{water}} := 3:1$ with distilled water under pressure, as described above. Residual concentrations of U(VI) were analysed.

The best U(VI) removal efficiencies ($\%R > 98\%$) very close in values were obtained at pH range 7.5–9.5, which may be explained by the physicochemical interactions of U(VI) species studied by sorption and/or precipitation with sorbent species generated in situ: $[\text{Fe}(\text{OH})_2]^+$, $\text{Fe}(\text{OH})_3$ and $[\text{Fe}(\text{OH})_4]^-$ plotted in Fig. 2. Wang et al.⁶⁴ have demonstrated that the sorbent's surface charge is influenced by aging⁶⁵ by its concentration and the zeta potential of the sorbents generated in situ is positive at pH around 8, then becomes negative⁶⁶.

U(VI) : sorbent dose, [U(VI)]: [Fe(III)]. The sorbent dose is important for the highly efficient removal of U(VI) species from diluted aqueous systems by sorption / flotation, the possible interactions being physical (sorption) or chemical (co-precipitation). The optimum amount of sorbent is a minimum of solid waste, but a maximum of adsorbent support that ensures maximum efficiency.

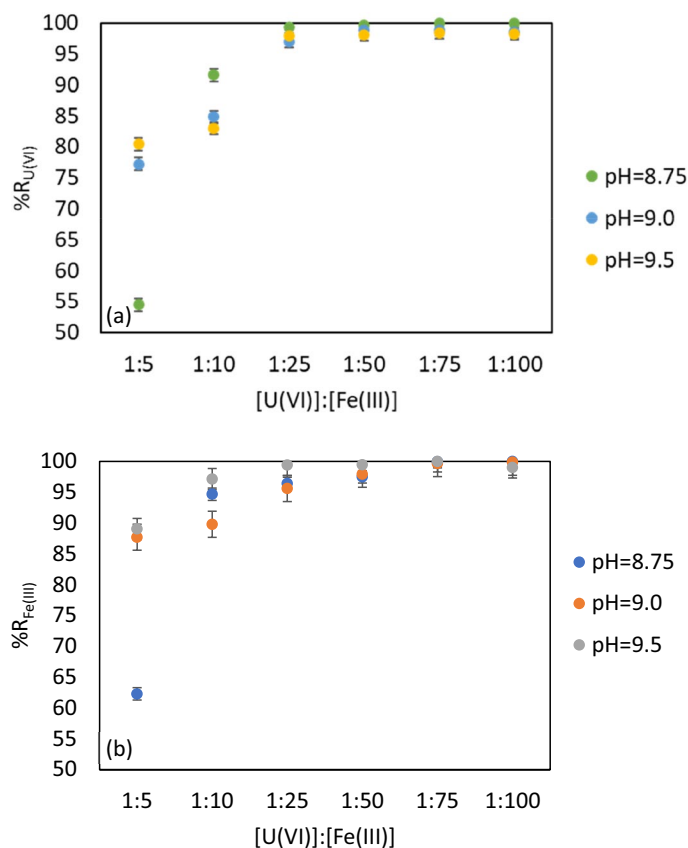


Figure 4. (a) $\%R_{U(VI)} = f([U(VI)] : [Fe(III)])$ in the optimal pH range; (b) $\%R_{Fe(III)} = f([U(VI)] : [Fe(III)])$ in the optimal pH range ($V_{\text{sample}} = 200$ mL, stirring rate 250 RPM, contact time 30 min, $p = 4 \times 10^5$ N·m⁻², dilution ratio $V_{\text{sample}} : V_{\text{water}} = 3:1$).

The different molar ratios [U(VI)]: [Fe(III)] ranging between 1: 5 and 1: 100 were provided using known volumes of 0.1 M and 0.01 M FeCl₃ solutions. The pH adjustments in the range 7.5–9.5 were made using 0.1 M and 0.01 M NaOH solutions. The studies were performed for the pH values 8.5, 9.0, and 9.5 (pH of real mine waters). Surfactant's concentration used was the same for all these experiments to provide the best solid phase separation. Figure 4a, b show the obtained results for the residual concentrations of U(VI) and Fe (III) and the recovery efficiency.

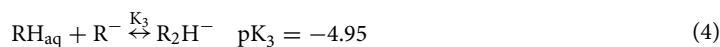
Lower molar ratios [U(VI)]: [Fe(III)] between 1:5 and 1:25 were not adequate because U(VI) concentrations exceed the legal limit at the international level⁶⁷. The sorbent—contaminant contact surface was not efficient for the removal of U(VI) according to the legislation in force.

The molar ratio [U(VI)]: [Fe (III)] = 1:75 and pH = 8.75, 9.0 and 9.5 corresponds to a maximum efficiency of U(VI) and Fe(III) removal, %R = 99.96% ($C_{U(VI)} = 0.0044$ mg·L⁻¹ and $C_{Fe(III)} = 0.01$ mg·L⁻¹ as mean value).

Molar ratio, [U(VI)]: [NaOL]. In the precipitate flotation, the surfactant consumption is substoichiometric molar ratio. However, the concentration is important because floatability should increase in terms of concentrations below the critical micellar concentration of the surfactant⁶⁸.

To provide the best separation of the sorbent loaded with U(VI), it is necessary to determine the optimal amount of NaOL, which increases the solid phase's hydrophobicity and floatability due to its long C-chain⁶³. Aqueous sodium oleate species are pH-dependent, therefore the same pH values were provided to run the experiments.

According to^{51,63} the chemical equilibria that should be considered between the oleate species are:



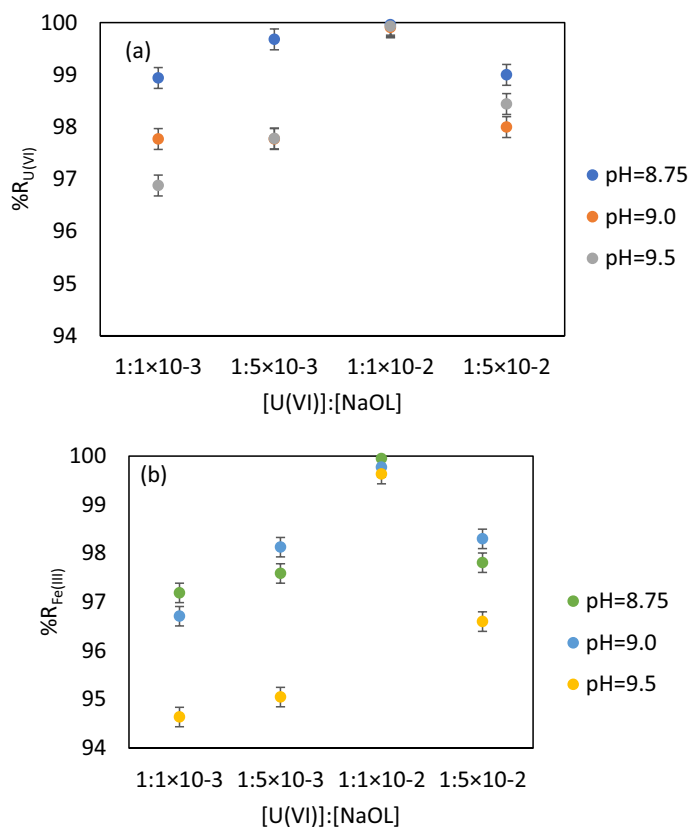
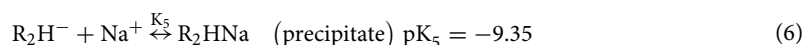


Figure 5. (a) $\%R_{U(VI)} = f([U(VI)] : [NaOL])$ in the optimal pH range; (b) $\%R_{Fe(III)} = f([U(VI)] : [NaOL])$ in the optimal pH range ($V_{\text{sample}} = 200$ mL, contact time 30 min., stirring rate 250 RPM, molar ratio $[U(VI)] : [Fe(III)] = 1 : 75$, $p = 4 \times 10^5$ N·m⁻², dilution ratio $V_{\text{sample}} : V_{\text{water}} = 3 : 1$).



where: RH is oleic acid; R⁻ is oleate ion; R₂H⁻ is acid-soap complex; R₂HNa is acid-soap salt and R₂²⁻ is oleate dimer, respectively.

The results of the experiments are showed in Fig. 5.

The results shown in Fig. 5 suggest that the most reliable molar ratio is $[U(VI)] : [NaOL] = 1 : 1 \times 10^{-2}$.

Contact time U(VI) with Fe (III) and NaOL. The contact time includes both the time required to prepare the sorbent in situ and the time of pH adjustment; the determined working pH value of 8.75 was in accordance with the literature data^{24,25,69} regarding the formation of the Fe₂O₃ · n H₂O precipitate within the limits 7.0–9.5 as shown in Fig. 2. %R values as a function of contact time are shown in Fig. 6.

It can be observed that after 30 min the removal efficiency (%R) reaches the maximum value of 99.96. An additional increase in contact time determines no variation in removal efficiency (%R = 99.96). Therefore, the chosen contact time was 30 min because any other higher value it is not justified.

Stirring rate. This factor is important in the sorption stage of U(VI) on the sorbent. High stirring velocities determine smaller sizes of sorbent flake and the decrease of the U(VI) removal efficiency.

Figure 7 points out that 250 RPM is the best stirring rate to get U(VI) and Fe (III) removal efficiencies > 98%.

The air pressure (p) in the pressurized water recipient. The air pressure in the pressurized water recipient of flotation cell ensures the formation of homogeneous bubbles capable of taking up the solid sorbent loaded with U(VI) and to ensure sufficient ascending force for the loaded sorbent to concentrate on the top of the flotation cell column. Therefore, a low air pressure does not ensure these conditions and favours the reverse process of depositing the loaded sorbent at the bottom of the flotation cell column^{48,49}. Higher air pressure values produce turbulence with a negative impact on the stability of aggregate bubble-loaded sorbent.

The results obtained and displayed in Fig. 8 suggests that the best working value of the air pressure is $p = 4 \cdot 10^5$ N·m⁻², when the removal efficiency is maximum: $\%R_{U(VI)} = 99.96$ and $\%R_{Fe(III)} = 99.95\%$, respectively.

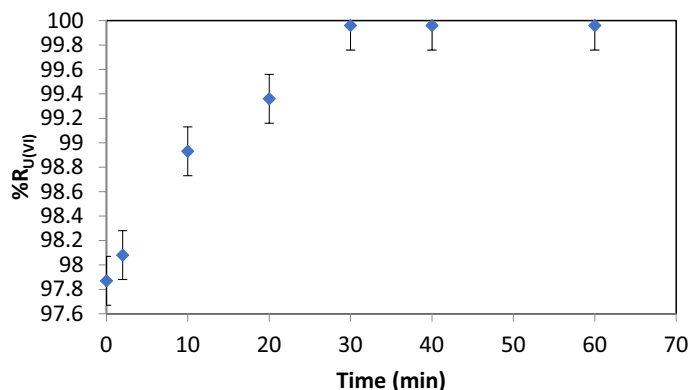


Figure 6. %R = f (contact time), $V_{\text{sample}} = 200$ mL, stirring rate 250 RPM, pH = 8.75, [U(VI)] : [Fe (III)] : [NaOL] = 1 : 75 : 1×10^{-2} , $p = 4 \times 10^5$ N·m⁻², dilution ratio $V_{\text{sample}} : V_{\text{water}} = 3 : 1$

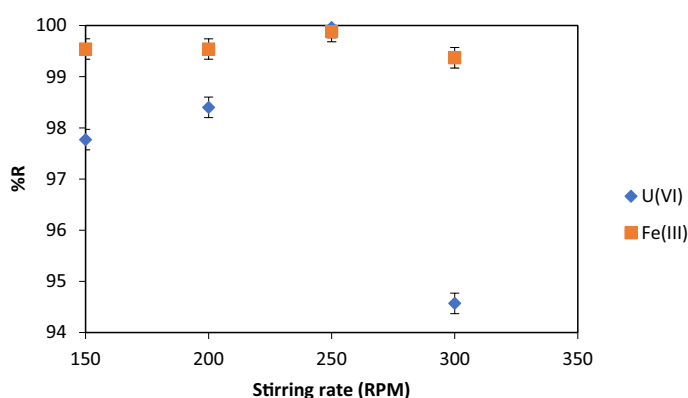


Figure 7. %R = f (stirring rate), $V_{\text{sample}} = 200$ mL, contact time 30 min, pH = 8.75, molar ratio [U(VI)] : [Fe (III)] : [NaOL] = 1 : 75 : 1×10^{-2} , $p = 4 \times 10^5$ N·m⁻², dilution ratio $V_{\text{sample}} : V_{\text{water}} = 3 : 1$

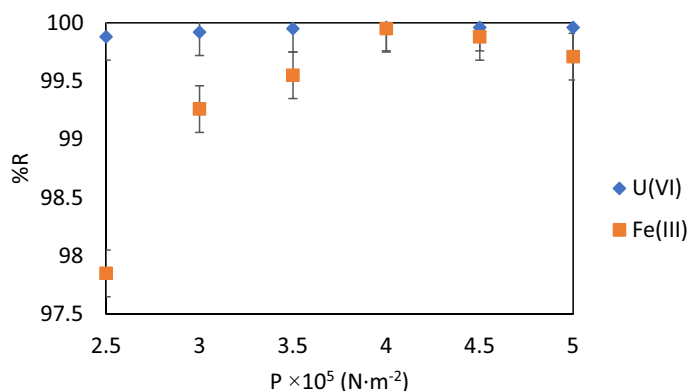


Figure 8. %R = f (p), $V_{\text{sample}} = 200$ mL, stirring rate 250 RPM, contact time 30 min, pH = 8.75, molar ratio [U(VI)] : [Fe (III)] : [NaOL] = 1 : 75 : 1×10^{-2} , $p = 4 \times 10^5$ N·m⁻², dilution ratio $V_{\text{sample}} : V_{\text{water}} = 3 : 1$

The U(VI) concentration. The variation of the concentration of contaminants has an important impact on the separation efficiency because it determines the consumption of reagents and the volume of loaded sorbent.

As such, when the concentration reaches high values, it increases the weight of the loaded sorbent and decreases the floatability of solid phase.

Figure 9 shows the effect of U(VI) concentration increase on the removal efficiency. Increases to 99.96% and then decreases slightly to concentrations greater than 20 mg·L⁻¹.

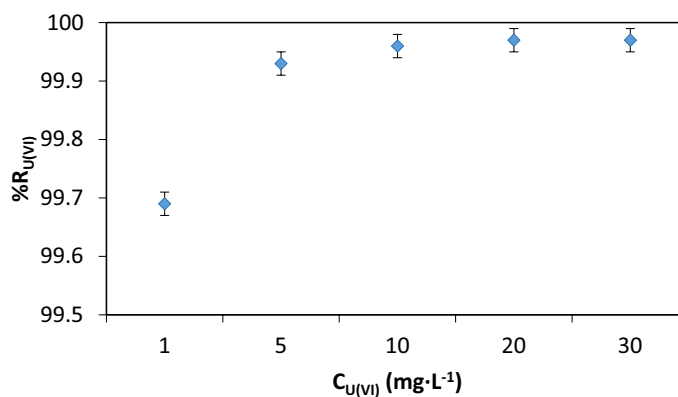


Figure 9. %R = f(U(VI)), $V_{\text{sample}} = 200 \text{ mL}$, stirring rate 250 RPM, contact time 30 min, pH = 8.75, molar ratio [U(VI)] : [Fe(III)] : [NaOL] = 1 : 75 : 1×10^{-2} , $p = 4 \times 10^5 \text{ N·m}^{-2}$, dilution ratio $V_{\text{sample}} : V_{\text{water}} = 3 : 1$

Optimum parameters. The optimal parameters (at maximum removal efficiency, %R) in order of the stages of the Sorption / Flotation process are:

- U(VI) concentration 10 mg L^{-1} ;
- Flotation pH range 7.5–9.5;
- U(VI) : sorbent dose, [U(VI)] : [Fe(III)] = 1: 75;
- Contact time U(VI) with Fe(III) = 25 min.;
- Stirring rate = 250 RPM;
- Molar ratio [U(VI)]: [NaOL] = 1: 1×10^{-2} ;
- Contact time U(VI) with Fe(III) and NaOL = 5 min.;
- Air pressure, $p = 4 \times 10^5 \text{ N m}^{-2}$;
- Flotation time = 5 min.

The accompanying heavy metals ions' interference. Seven samples ($V_{\text{sample}} = 200 \text{ mL}$) were prepared in which U(VI), Cu(II), Cr(VI), and Mo(VI) were introduced 10 mg·L^{-1} each, were subjected to sorption / precipitate flotation under the optimal values of the previously established working parameters in order to observe the interactions between all ionic species. The results suggest that, in the multi-component solution, Cu(II) and Fe(III) precipitate, and U(VI) could be sorbed and/or precipitated. The Mo(VI) and Cr(VI) species can also be sorbed on $\text{Fe}_2\text{O}_3 \cdot n \text{ H}_2\text{O}$ generated in situ.

In the case of Cu(II), the obtained results suggest that at working pH = 8.75 it precipitates as Cu(OH)_2 ^{49,70–72}.

The precipitates' formation takes place in the order from the lowest to the most soluble product, i.e. Fe(OH)_3 ($K_{\text{sp}} = 2.79 \times 10^{-39}$) < $\text{UO}_2(\text{OH})_2$ ($K_{\text{sp}} = 1.1 \times 10^{-20}$) < UO_2CO_3 ($K_{\text{sp}} = 1.8 \times 10^{-12}$) < CuCO_3 ($K_{\text{sp}} = 1.4 \times 10^{-10}$)^{49,60,61,70–72}, according to the previously stated principle (3.1.1).

The main speciation of Cr(VI) at working pH = 8.75 is CrO_4^{2-} according to the literature^{73,74}.

In the case of Mo(VI) species, the researchers pointed out that the probable main speciation is MoO_4^{2-} with a maximum concentration value at pH = 7, when the concentrations of the other two, H_2MoO_4 and HMoO_4^- , are very low⁷⁵.

Figure 10 shows the influence of the accompanying ions on U(VI) removal by sorption / precipitate flotation. It can be observed that, when Cu(II) and Mo(VI) species accompany U(VI) in bicomponent systems, the sorption U(VI) is not influenced by them unlike the case of Cr(VI), which decreases the removal efficiency of U(VI).

It can also be observed that following the sorption / precipitate flotation process, the removal efficiency of U(VI) from these studied aqueous systems is very high (%R > 99) considering that in solution the residual concentration of U(VI) has values in range $0.1\text{--}1.9 \mu\text{g·L}^{-1}$ which are much lower than the maximum permitted legal limit concentration (0.02 mg·L^{-1}) stipulated by WHO regulations.

Other research studies presenting interactions in the aqueous species of U(VI) and the heavy metals accompanying of sorbent generated in situ have pointed out dominant metallic ionic speciation in the dilute aqueous systems, which are similar to those studied.

Riba et. al. has showed that for a solution with [U(VI)] = 4.2 mM (10 mg·L^{-1}) in contact with 1.2% $\text{O}_2(\text{g})$ and 0.017% $\text{CO}_2(\text{g})$ for a pH range of 8 to 9 the dominant species are $[\text{UO}_2(\text{CO}_3)_3]^{4-}$ and $[\text{UO}_2(\text{CO}_3)_2]^{2-}$ ²⁵.

Wanze et.al. has pointed out for [U(VI)] = $4.2 \times 10^{-6} \text{ M}$ dissolved in 0.01 M NaCl solution in the presence of carbonate $[\text{CO}_3^{2-}] = 1 \times 10^{-2} \text{ M}$ there are the same dominant speciations⁶⁹.

The presence of $[\text{MoO}_4^{2-}]$ was demonstrated by Mitchell in the system with [Mo(VI)] = 0.3 and 1 mM (3 mg/L and 100 mg/L) at a pH range 2 to 7⁷⁵.

According to Matis and Mavros in a diluted aqueous system containing Cu(II) = 10 mg/L at pH range 8 to 10 precipitates Cu(OH)_2 ³³.

For [Cr(VI)] between 10^{-4} and $6 \times 10^{-4} \text{ M}$ in the pH range 1 to 12, the dominant speciation is CrO_4^{2-} ^{74,76}.

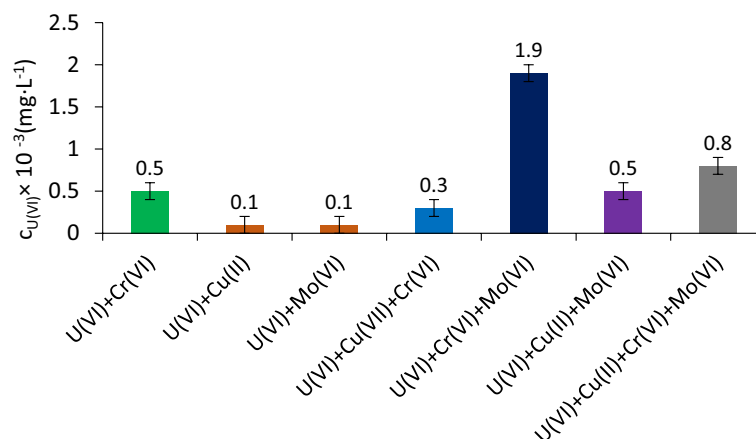


Figure 10. Influence of accompanying metallic ionic species $C_i = 10 \text{ mg}\cdot\text{L}^{-1}$ on the variation of U(VI) content in the aqueous diluted systems after sorption / precipitate flotation.

The results obtained demonstrate the presence of a competition between the metallic ion ionic species present in order to bind to the active surface of the sorbent charge with electric charge⁷⁴. Since the zero sorption point of sorbent changes with increasing amount of $\text{Fe}_2\text{O}_3 \cdot n \text{ H}_2\text{O}$ ⁶⁴, the obtained results suggest that Cu (II) species precipitate and Cr (VI) and Mo (VI) are removed from aqueous solution by sorption. The experimental results point out that it is possible that U(VI) is electrostatically bound to the electrically charged surface of the sorbent as a carbonate complex.

Experimental results prove that the accompanying heavy metals do not significantly influence the separation efficiency.

From the study of influencing factors correlated with the maximum efficiency of U(VI) separation, it results that the optimal working parameters of U(VI) separation by sorption / precipitate flotation are: pH range 7.0–9.5, stirring rate 250 RPM, contact time 30 min, molar ratio $[\text{U(VI)}] : [\text{Fe(III)}] : [\text{NaOL}] = 1 : 75 : 1 \times 10^{-2}$, $p = 4 \cdot 10^5 \text{ N}\cdot\text{m}^{-2}$, dilution ratio $V_{\text{sample}} : V_{\text{water}} = 3 : 1$, flotation time 5 min, depending on initial concentration range of U(VI) = 1–30 $\text{mg}\cdot\text{L}^{-1}$.

The optimum working conditions established for the synthetic aqueous systems were validated on real mine water samples and very good results have been obtained.

The interaction of sorbent with U(VI) and the accompanying heavy metals. Preliminary data on the interaction between U(VI) and sorbent were obtained using the FT-IR spectra analysis of two samples obtained under optimal working conditions for sorption / precipitate flotation Sample 1— $\text{Fe}_2\text{O}_3 \cdot n\text{H}_2\text{O}$ and Sample 2— $\text{Fe}_2\text{O}_3 \cdot n\text{H}_2\text{O}$ with U(VI) carbonated complex.

Both spectra include the 3400 cm^{-1} IR band that can be assigned to the stretching modes of H_2O molecules or the coating of hydrogen-bonded surface OH groups, while the 3037 cm^{-1} IR band is due to the presence of OH stretching mode in $\alpha\text{-FeOOH}$ and a corresponding prominent peak H_2O coordinated or adsorbed close to 1620 cm^{-1} ⁷⁷.

The U(VI) carbonate complex's ions fixing on the adsorbent seems to be emphasized by the movement which is observed from 653 cm^{-1} to 626 cm^{-1} in Sample 2. The claim appears to be supported by the positive potential value near $\text{pH} = 8.0$ ⁶⁶.

Table 1 presents the characteristic bands attributed to the sublates obtained after the U(VI) separation from Cr(VI), Cu(II), and Mo(VI) by sorption/precipitate flotation.

All FT-IR spectra with the characteristic bands shown in Table 1 present the following specific peaks:

- In the $3000\text{--}3650 \text{ cm}^{-1}$ range are attributed to associated and non-associated hydroxyl groups;
- In the $1620\text{--}1634 \text{ cm}^{-1}$ range attributed to the water adsorbed on the in situ generated $\text{Fe}_2\text{O}_3 \cdot n\text{H}_2\text{O}$ surface;
- The characteristic bands around 1500 cm^{-1} value attributed to the carbonate ions stretching vibration, which are present for *I* (Fe(III)) at 1486 cm^{-1} , for *A* (Fe(III) + U(VI)) at 1521 cm^{-1} , for *B* (Fe(III) + U(VI) + Cr(VI)) at 1542 cm^{-1} , for *C* (Fe(III) + U(VI) + Cu(II)) at 1512 cm^{-1} , for *E* (Fe(III) + U(VI) + Mo(VI)) at 1518 cm^{-1} , for *D* (Fe(III) + U(VI) + Cr(VI) + Cu(II)) with shoulder at 1519 cm^{-1} , for *F* (Fe(III) + U(VI) + Cr(VI) + Mo(VI)) with shoulder at 1540 cm^{-1} , for *G* (Fe(III) + U(VI) + Cu(II) + Mo(VI)) with shoulder at 1526 cm^{-1} and for *H* (Fe(III) + U(VI) + Cr(VI) + Cu(II) + Mo(VI)) at 1512 cm^{-1} ;
- The characteristic bands around 1400 cm^{-1} value may be attributed to the deformation vibration bond of FeOOH and they are present in all samples except sample *I* (Fe(III)) suggesting that U(VI), Cr(VI), and Mo(VI) might be bonded on the sorbent surface and that Cu(II) might be precipitated as copper carbonate at the working pH;
- The characteristic bands at 703 cm^{-1} attributed $\nu_{\text{Fe-O}}$ is present in *A* (Fe(III) + U(VI)) and *B* (Fe(III) + U(VI) + Cr(VI)) samples and seems to suggest the possibility of U(VI) bonding on the in situ generated sorbent;

Characteristic bands, cm ⁻¹									Characteristic bands attribution	References
Sample I	Sample A	Sample B	Sample C	Sample E	Sample D	Sample F	Sample G	Sample H		
3609-3305 3037	3609-3305 3037	3609-3305 3037	3679-3218 3048	3692-3246 3034 (s)	3685-3212 3041	3685-3233 3048	3685-3233 3048	3678-3240 3048 (s)	v _{OH non-assoc} v _{OH assoc} v _{HOH}	78-81
2854 2728	2854 2728	2854 2724	2857 2729	2850 2701	2850 2723 1964	2843 2715 2347	2843 2715 2347	2850 2701 2347	v _{CH}	80
1634	1620	1634	1632	1639	1639	1632	1639	1639	δ _{OH} , δ _{HOH}	79,81
1486*	1521	1542 1493*	1512 1335*	1518 1327*	1519 (s) 1328*	1540 (s) 1306*	1526 (s) 1328*	1512 1327*	v _{CO₃²⁻} v _{COO⁻}	80,82
1000-800	-	957 858	903	-	-	-	-	-	δ _{CO₃²⁻}	80,82
^b 682 ^b 647 ^b 612	^a 703 626	^a 703 ^a 619	^d 683	^d 690	^f 669	^d 683	676	669	^{a, b} (v _{Fe-O} , δ _{Fe-O}) ^c Fe-CO in the same plane complex [(UO ₂) ₂ (OH) ₂] ²⁺ + CO ₃ ²⁻ ^f v _{Cu-O} , δ _{Cu-O}	83-85
569 534	556 527	534	506	541	556 506	542	542	563	v _{Fe-O}	79,83,84
499 463	478	485	414	470		428	421	470	δ _{Fe-O}	79,86-88

Table 1. Characteristic bands of sublates obtained after the separation by sorption/precipitate flotation of U(VI) from Cr (VI), Cu(II), and Mo(VI). Where : Sample I = Fe₂O₃·nH₂O symbolized as Fe (III); Sample A = Fe(III) + U(VI); Sample B = Fe(III) + U(VI) + Cr(VI); Sample C = Fe(III) + U(VI) + Cu(II); Sample E = Fe(III) + U(VI) + Mo(VI); Sample D = Fe(III) + U(VI) + Cr(VI) + Cu(II); Sample F = Fe(III) + U(VI) + Cr(VI) + Mo(VI); Sample G = Fe(III) + U(VI) + Cu(II) + Mo(VI); Sample H = Fe(III) + U(VI) + Cr(VI) + Cu(II) + Mo(VI).

- The characteristic bands at 682 cm⁻¹, 647 cm⁻¹, and 612 cm⁻¹ attributed to δ_{Fe-O} from sample I (Fe (III)) seem to point out the available active sites' existence for U(VI) and accompanying elements ions bonding;
- The band characteristic to the complex [(UO₂)₂(OH)₂]²⁺ + CO₃²⁻ appears only in the systems : C(Fe(III) + U(VI) + Cu(II)) at 683 cm⁻¹; E(Fe(III) + U(VI) + Mo(VI)) at 690 cm⁻¹ and F(Fe(III) + U(VI) + Cr(VI) + Mo(VI)) at 683 cm⁻¹;
- The bands δ_{Fe-O} and v_{Fe-O} are also shifted towards lower values indicating that chemisorption might be possible at this level as well.

The FT-IR spectra analysis suggests that there is a possibility for the [(UO₂)₂(OH)₂]²⁺CO₃²⁻ complex's formation considering that the reaction kinetics is of pseudo-second-order involving the chemisorption. At the same time at the working pH, Cu (II) can precipitate, and Cr (VI) and Mo (VI) to be adsorbed on the Fe (III) oxyhydroxide^{50,74}.

Table 2 shows the sublates' thermal analysis' results obtained after the separation by sorption/precipitate flotation of U(VI) from Cr (VI), Cu (II), and Mo (VI).

The analysis of TG/DTG/DTA curves shows the sublates' non-iso-thermal degrading process in the air atmosphere in the case of the bi-, three- and tetra component systems. The samples were subjected to three successive decomposing and water loss processes (Table 2).

The first endothermic process (20–120 °C) points out moisture's complete loss. The analysed samples present similar moisture. The weight losses in this stage are about Δm₁ = 4.57–6.21% at the maximum temperatures within the range 97.1–109.3 °C.

The samples seem to be stable within the temperature range of 120–250 °C. Then the second decomposition process follows, which is exothermic (250–350 °C) and represents the main degrading stage with the weight loss Δm₂ = 6.14–8.07% at the maximum temperatures within the ranges 273.0–281.0 °C and 304.1–347.5 °C, respectively.

At higher temperatures (350–900 °C) the last exothermic process of thermal-oxidative decomposition of non-volatile products was obtained in the second degrading stage.

In all cases for the temperatures ranging within 513.7–620.9 °C the similar residual weights Δm₃ = 1.35–2.06% point out the studied metallic ions' oxides' mixtures' occurrence.

Reproducibility and optimal parameters validation on real mine water samples. *Reproducibility of U(VI) removal by sorption/precipitate flotation.* Previously determined sorption/precipitate flotation technique optimal parameters were examined on 10 identical sample solutions (C₀ = 10 mg/L) corresponding to two different molar ratios ([U(VI)] : [Fe (III)] : [NaOL] = 1 : 75 : 1 × 10⁻² and 1 : 100 : 1 × 10⁻²), respectively, to calculate the U(VI) removal reproducibility by Student method (Table 3).

Optimal parameters validation on real mine water samples. The mine water samples (MW1-MW3) were collected from a former uranium mining site in the Banat region and their chemical composition is shown in

Sample	DTA			
	Temperature domain (°C)	$\pm \Delta m$ (%)	Maximum temperature DTA (°C)	Reaction type
Fe ₂ O ₃ ·nH ₂ O is symbolized as Fe (III)	20–120	–5.65	97.1	Endo
	120–350	–8.07	304.1	Exo
	350–800	–2.27	620.9	Exo
	800–900	–1.54	–	–
Fe (III) + U(VI)	20–120	–5.09	100.7	Endo
	120–350	–6.34	277.2 341.3	Exo Exo
	350–900	–1.48	513.7	Exo
Fe (III) + U(VI) + Cr (VI)	20–120	–4.57	108.8	Endo
	120–350	–6.62	273.3 347.5	Exo Exo
	350–900	–1.38	598.7	Exo
Fe (III) + U(VI) + Cu (II)	20–120	–6.21	107.6	Endo
	120–350	–6.96	275.8 346.2	Exo Exo
	350–900	–1.99	593.9	Exo
Fe (III) + U(VI) + Mo (VI)	20–120	–6.17	102.3	Endo
	120–350	–6.14	273.0 340.2	Exo Exo
	350–900	–1.42	536.9	Exo
Fe (III) + U(VI) + Cr (VI) + Cu (II)	20–120	–5.81	109.3	Endo
	120–350	–6.80	278.0	Exo
	350–900	–2.06	533.8	Exo
Fe (III) + U(VI) + Cr (VI) + Mo (VI)	20–120	–5.51	103.7	Endo
	120–350	–6.27	281.0 344.7	Exo Exo
	350–900	–1.35	555.3	Exo
Fe (III) + U(VI) + Cu (II) + Mo (VI)	20–120	–5.36	105.7	Endo
	120–350	–6.74	277.1 349.0	Exo Exo
	350–900	–1.86	586.2	Exo
Fe(III) + U(VI) + Cr(VI) + Cu(II) + Mo(VI)	20–120	–6.22	103.8	Endo
	120–350	–6.57	276.9 342.9	Exo Exo
	350–900	–1.55	549.2	Exo

Table 2. The thermal analysis of sublates obtained after the separation by sorption/precipitate flotation of U(VI) from Cr (VI), Cu (II), and Mo (VI).

Table 4. They were processed according to the proposed flowsheet (Fig. 12) with and without pH adjustment respectively. The pH was adjusted with 0.1 M HCl solution to the working value of 8.75.

It was observed that the U(VI) removal efficiency was higher after pH adjustment, so that the sorption flotation was very efficient (Fig. 11).

Figure 12 summarizes a proposed technological processing diagram (flowsheet) of the multi-contaminated aqueous system by sorption flotation.

In case the samples were processed without pH adjustment the separation efficiencies were 96.6% for sample MW1 and 97.2 for MW2 and MW3 samples, respectively (Fig. 13).

In case the samples were processed with pH adjustment at pH = 8.75 with 0.1 M HCl solution %R_{U(VI)} > 99 was obtained for MW1C–MW3C samples (Fig. 13).

One can note that U(VI) removal efficiency was higher for the pH-adjusted samples than for the others, confirming the optimal values of the previously studied parameters.

The generated solid waste may be stored or recycled as a U(VI) secondary source for the manufacture of nuclear fuel.

The optimal parameters validation of tandem process immobilization on NMS-flotation on real water samples was performed in two variants:

- Without pH adjustment and sorbent addition:** The real water samples with the chemical composition shown in Table 4 (300 mL) MW1–MW3 were pre-treated with 0.15 g NMS and were contacted for 30 min under 250 RPM stirring. The solid phase was separated by decantation. To the resulting liquid phase, MW1–MW3i, the appropriate amount of 0.25×10^{-3} M NaOL solution was added and floated without pH adjust-

No	Floated sample characteristics	C_p (mg·L ⁻¹)	Statistical probability
1	$C_o = 10 \text{ mg·L}^{-1}$ $V_{\text{sample}} = 200 \text{ mL}$ $\text{pH} = 8.75$ $[\text{U(VI)}] : [\text{Fe (III)}] : [\text{NaOL}] = 1 : 100 : 1 \times 10^{-2}$ $V_{\text{sample}} : V_{\text{water}} = 3 : 1$ $p = 4 \cdot 10^5 \text{ N·m}^{-2}$	0.01	$\bar{X} = 0.008$ $S = 2.6667 \cdot 10^{-6}$ $S_{\bar{X}} = 8.4328 \cdot 10^{-6}$ $P = 95\%$ $tS_{\bar{X}} = 0.000018$ $C_t = 0.008 \pm 0.000018$ $P = 99\%$ $tS_{\bar{X}} = 0.000032$ $C_t = 0.008 \pm 0.000032$
2		0.009	
3		0.008	
4		0.005	
5		0.007	
6		0.008	
7		0.006	
8		0.01	
9		0.009	
10		0.008	
11	$C_o = 10 \text{ mg·L}^{-1}$ $V_{\text{sample}} = 200 \text{ mL}$ $\text{pH} = 8.75$ $[\text{U(VI)}] : [\text{Fe (III)}] : [\text{NaOL}] = 1 : 75 : 1 \times 10^{-2}$ $V_{\text{sample}} : V_{\text{water}} = 3 : 1$ $p = 4 \cdot 10^5 \text{ N·m}^{-2}$	0.0044	$\bar{X} = 0.00426$ $S = 2.593 \cdot 10^{-4}$ $S_{\bar{X}} = 8.19998 \cdot 10^{-5}$ $P = 95\%$ $tS_{\bar{X}} = 0.00018285$ $C_t = 0.00426 \pm 0.00018285$ $P = 99\%$ $tS_{\bar{X}} = 0.000259939$ $C_t = 0.00426 \pm 0.000259939$
12		0.0043	
13		0.0040	
14		0.0044	
15		0.0039	
16		0.0041	
17		0.0045	
18		0.0040	
19		0.0046	
20		0.0044	

Table 3. Reproducibility of U(VI) removal by sorption/precipitate flotation. \bar{X} mean of the samples. S standard deviation of one measurement. $S_{\bar{X}}$ standard deviation of the mean. C_t U(VI) concentration after flotation. P probability that C_t be within a range of values. t t (Student) variable.

Sample	pH at 22 °C	U	Mo	Sn	Zn	Pb	Cr (VI)	Co	Cu	Ni	Na ₂ CO ₃	NaHCO ₃
MW1	9.43	13.8	0.264	<0.001	0.01	<0.001	<0.001	0.01	<0.001	<0.001	642.3	1527.1
MW2	9.59	10.35	0.284	<0.001	<0.001	<0.001	<0.001	0.01	<0.001	<0.001	749.4	1527.1
MW3	9.64	16.40	0.270	<0.001	<0.001	<0.001	0.01	<0.001	<0.001	<0.001	642.3	1527.1

Table 4. Chemical composition of real water samples (mg·L⁻¹).

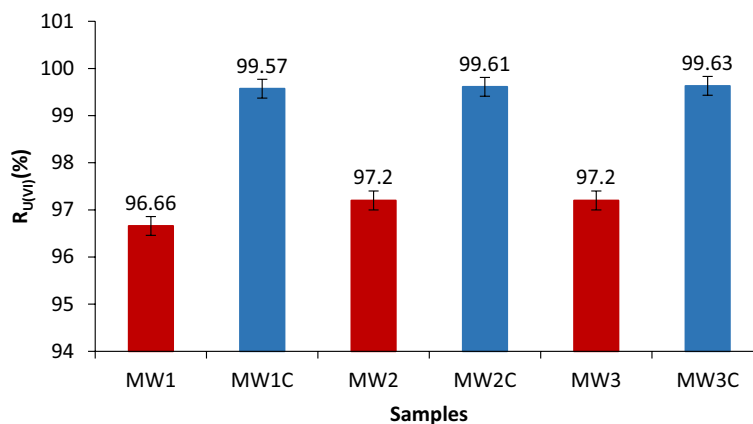


Figure 11. %R_{U(VI)} = f (pH adjustment), $V_{\text{sample}} = 200 \text{ mL}$, stirring rate 250 RPM, contact time 30 min, molar ratio $[\text{U(VI)}] : [\text{Fe (III)}] : [\text{NaOL}] = 1 : 75 : 1 \times 10^{-2}$, $p = 4 \times 10^5 \text{ N·m}^{-2}$, dilution ratio $V_{\text{sample}} : V_{\text{water}} = 3 : 1$, where ■ MW1–MW3—samples without pH adjustment and ■ MW1C–MW3C—samples with pH adjustment.

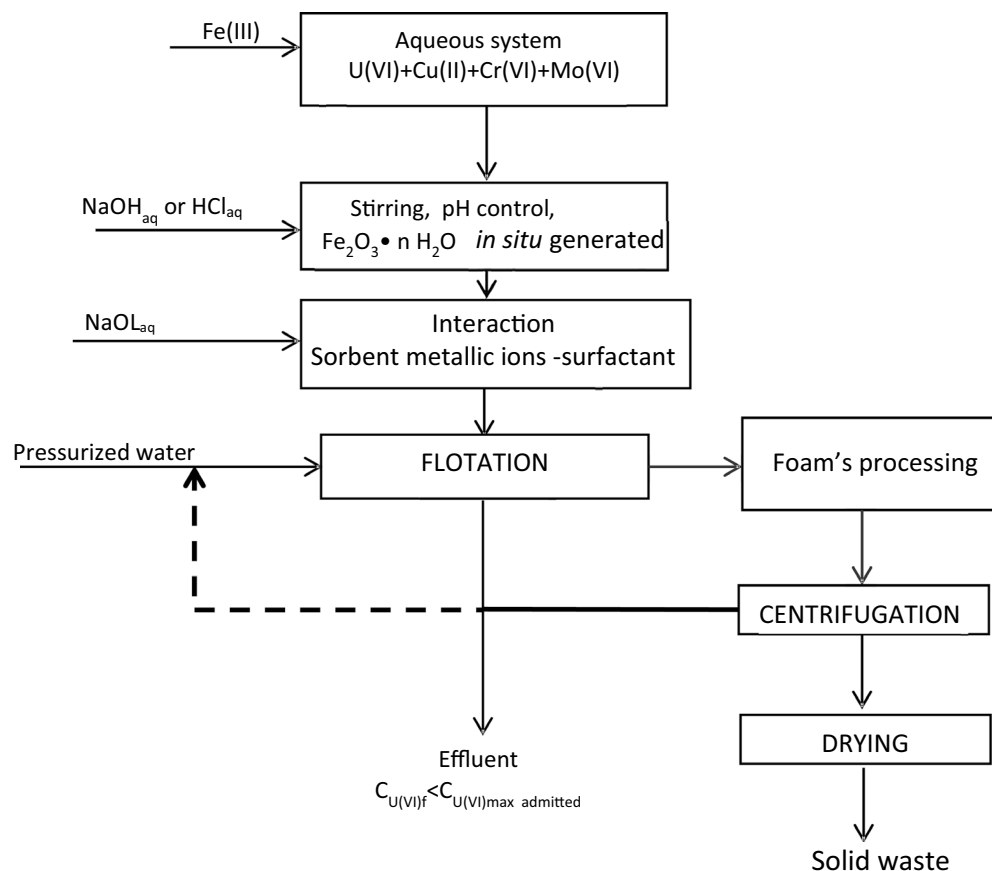


Figure 12. The separation scheme for the treatment of a multi-component system by sorption flotation adapted to the studied system⁵¹.

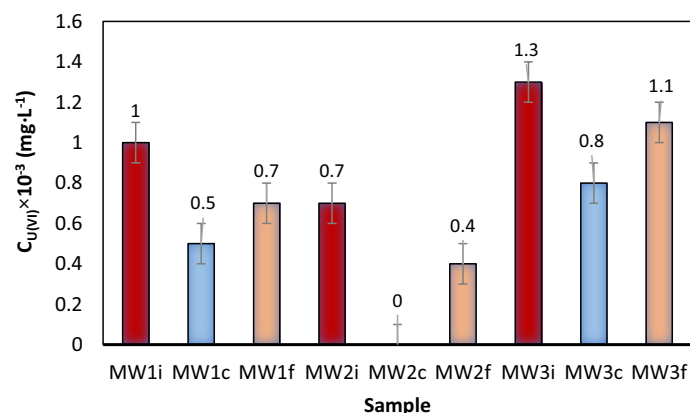


Figure 13. U(VI) residual concentration change in three real water samples after immobilization—sorption / flotation processing, where: ■ MW1i–MW3i is the liquid phase resulting after immobilization on NMS; ■ MW1c–MW3c is a liquid phase with pH adjusted with FeCl_3 0.1 ; ■ MW1f.–MW3f. is the liquid phase resulting after the immobilization on NMS, decantation, collector addition, and flotation.

ment and without addition of FeCl_3 0.1 M because the Fe^{2+} and Fe^{3+} supplied by the NMS in the filtered solution was used as an adsorption support. After flotation, the water samples MW1f.–MW3f. were obtained (Fig. 14).

- b. **With pH adjustment and sorbent addition:** The real water samples with the chemical composition shown in Table 4 (300 mL) MW1–MW3 were pre-treated with 0.15 g NMS for 30 min under 250 RPM stirring. The solid phase was separated by decantation. To the resulting liquid phase, MW1i–MW3i, the pH was adjusted

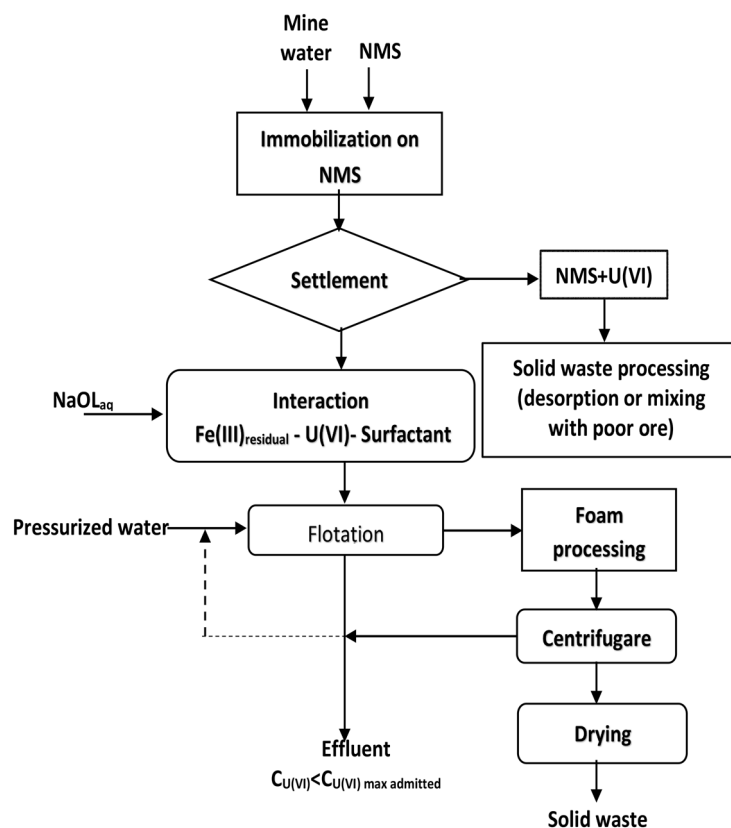


Figure 14. Immobilization and flotation without pH adjustment and in situ generated $\text{Fe}_2\text{O}_3 \cdot n\text{H}_2\text{O}$ using only the $\text{Fe(III)}_{\text{residual}}$ after U(VI) immobilization on NMS.

using 0.1 M FeCl_3 solution to avoid the addition of the foreign ion, the appropriate amount of 0.25×10^{-3} M NaOL solution was added and after flotation samples, MW1c–MW3c were obtained (Fig. 15).

Figure 13 shows the U(VI) residual content after immobilization and flotation of real water samples.

Two separation schemes' versions, which use both U(VI) removal methods, have resulted as follows: one without pH adjustment and without in situ generation of $\text{Fe}_2\text{O}_3 \cdot n\text{H}_2\text{O}$ (Fig. 14) and another one with pH adjustment and with in situ $\text{Fe}_2\text{O}_3 \cdot n\text{H}_2\text{O}$ generated (Fig. 15).

The obtained results on the real water samples suggest that U(VI) separation by sorption/precipitate flotation may be used either as a single method or as an additional stage in the case when Fe^0 -based nanomaterials are used in situ.

Conclusions

This paper studied the possibility of removing U(VI) and some associated metallic ions, specific to multicomponent aqueous systems in the uranium industry, by an efficient removal process as sorption on sorbent generated in situ ($\text{Fe}_2\text{O}_3 \cdot n\text{H}_2\text{O}$) followed by flotation ($\%R_{\text{U(VI)}}$ and $\%R_{\text{Fe(III)}} > 99$) in working conditions ($C_{\text{i,U(VI)}} = 10 \text{ mg} \cdot \text{L}^{-1}$, pH range = 7.5–9.5, $[\text{U(VI)}] : [\text{Fe(III)}] = 1 : 75$, contact time = 30 min., stirring rate = 250 RPM, $[\text{U(VI)}] : [\text{NaOL}] = 1 : 1 \times 10^{-2}$, $p = 4 \times 10^5 \text{ N} \cdot \text{m}^{-2}$, flotation time = 5 min.).

In establishing the separation process, the existing speciations, possible interactions and probable species participating in the process (pH range 7.0–9.5) were taken into account: U(VI) hydroxide complex ($\text{UO}_2(\text{OH})_2$, $[\text{UO}_2(\text{OH})_3]^-$ and $[(\text{UO}_2)_3(\text{OH})_7]^-$), U(VI) carbonate complexes (UO_2CO_3 , $[\text{UO}_2(\text{CO}_3)_2]^{2-}$, $[\text{UO}_2(\text{CO}_3)_3]^{-4}$ and $[(\text{UO}_2)_2\text{CO}_3(\text{OH})_3]^-$), Fe(III) hydroxide complex ($\text{Fe}_2\text{O}_3 \cdot n\text{H}_2\text{O}$).

To explain the separation mechanism were registered: FTIR spectra (range 400–4000 cm^{-1}) and derivatograms (range 20–1000 °C) of the solid loaded with U(VI) concentrated in foam (sublate). Thus FT-IR analysis has pointed out the possibility of forming the complex $[(\text{UO}_2)_2(\text{OH})_2]^{2+}\text{CO}_3^{2-}$, which may be bond to Fe(III) oxyhydroxides formed at upon immobilization on NMS and (in case of the flotation process in tandem by pre-treated of aqueous systems with the immobilization on Fe-based nanomaterials) / or generated in situ $\text{Fe}_2\text{O}_3 \cdot n\text{H}_2\text{O}$ sorbent formed in precipitate flotation process, as well.

In the case of applying the proposed procedure on real samples pre-treated with NMS (Fe^0 based nanomaterial), without pH adjustment and FeCl_3 addition, the solid phase loaded with metallic ions was separated by decantation. The separation efficiency was more than 99%.

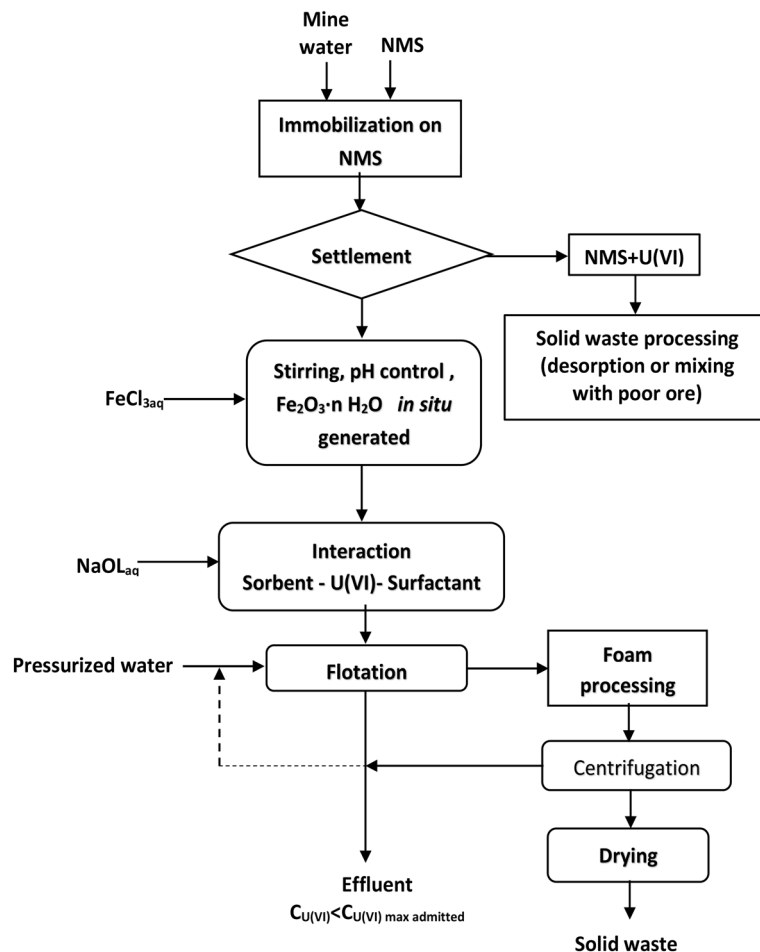


Figure 15. Immobilization and flotation where for pH adjustment 0.1 M FeCl_3 solution is used, which is the reagent for sorbent in situ generation.

In the case of applying the proposed procedure on real samples pre-treated with NMS (Fe^0 based nano-material), with pH adjustment and FeCl_3 addition, the solid phase loaded with metallic ions was separated by decantation. The pH of the aqueous phase after settling is adjusted to $\text{pH} = 8.75$ by adding FeCl_3 solution. The adsorbent is generated in situ, it will be loaded with metallic ions remaining from their immobilization on the NMS and finally flotation stage is applied. The separation efficiency was more than 99%.

Validation of optimal parameters on multicomponent real mine water samples and the ability of $\text{Fe}_2\text{O}_3 \cdot n\text{H}_2\text{O}$ to interact with multiple metallic speciations concludes that sorption/precipitate flotation tandem could be considered an advantage complementary in remediation technology, as a novelty in this area.

Data availability

The datasets used and/or analyzed during the current study are available from the corresponding author upon reasonable request.

Received: 11 March 2022; Accepted: 23 August 2022

Published online: 10 October 2022

References

- Crane, R. A., Dickinson, M., Popescu, I. C. & Scott, T. B. Magnetite and zero-valent iron nanoparticles for the remediation of uranium-contaminated environmental water. *Water Res.* **45**, 2391–2942 (2011).
- Bielicka, A., Bojanowska, I. & Wiśniewski, A. Two faces of chromium-pollutant and bioelement. *Pol. J. Environ. Stud.* **14**(1), 5–10 (2005).
- Newsome, L., Morris, K. & Lloyd, R. The biogeochemistry and bioremediation of uranium and other priority radionuclides. *Chem. Geol.* **363**, 164–184 (2014).
- Polat, H. & Erdogan, D. Heavy metal removal from wastewaters by ion flotation. *J. Hazard. Mater.* **148**(1–2), 267–273 (2007).
- Crane, R. A., Pullin, H. & Scott, T. B. The influence of calcium, sodium, and bicarbonate on the uptake of uranium onto nanoscale zero-valent iron nanoparticles. *Chem. Eng. J.* **277**, 252–259 (2015).
- Kurniawan, T. A., Chan, G. Y. S., Lo, W.-H. & Babel, S. Physicochemical treatment techniques for wastewater laden with heavy metals. *Chem. Eng. J.* **118**(1–2), 83–98 (2006).

7. Aydin, F. A. and Soylak, M. A novel multi-element co-precipitation technique for separation of metal ions in environmental samples, *Talanta* 134–141 (2007)
8. Chengrouche, M. S. & Barakat, M. The precipitation of ammonium uranyl carbonate (AUC): thermodynamic and kinetic investigations. *Hydrometallurgy* 85, 163–171 (2007).
9. Fu, F. & Wang, Q. Removal of heavy metals ions from wastewaters: a review. *J. Environ. Manag.* 92, 407–418 (2011).
10. Wang, L. K., Vaccari, D. A., Li, Yang, Shammam, N. K. 2005, Cap.5 Chemical Precipitation in Handbook of Environmental Engineering, Volume 3: Physicochemical Treatment Processes Edited by: L. K. Wang, Y.-T. Hung, and N. K. Shammam © The Humana Press Inc., Totowa, NJ, 143–197.
11. Anirudhan, T. S. & Radhakrishnan, P. G. Improved performance of a biomaterial-based cation exchanger for the adsorption of uranium (VI) from water and nuclear industry wastewater. *J. Environ. Radioact.* 100, 250–257 (2009).
12. Khalifa, M. E. Selective separation of uranium using Alizarin Red S (ARS)-Modified anion-exchange resin or by flotation of U-ARS chelate. *Sep. Sci. Technol.* 33(14), 2123–2141 (1998).
13. Ritcey, G.M., and Ashbrook, A.W. Solvent Extraction. Principles and Applications to Process Metallurgy, Elsevier, Amsterdam (1984)
14. Yonghui, Y. *et al.* Extraction of uranium (VI) through reversed micelle by primary amine N₁₉₂₃. *J. Radioanal. Chem.* 222(1–2), 239–241 (1997).
15. Anirudhan, T. S. & Rejith, S. Synthesis and characterization of carboxyl terminated poly (methacrylic acid) grafted chitosan/bentonite composite and its application for the recovery of uranium (VI) from aqueous media. *J. Environ. Radioact.* 106, 8–19 (2012).
16. Demirel, N., Merdivan, M., Pirinccioglu, N. & Hamami, C. Thorium (IV) and uranium (VI) sorption studies on octa carboxymethyl-C-methylcalix[4] resorcinarene impregnated on a polymeric support. *Analytica Chimica Acta* 485, 213–219 (2003).
17. Muzzarelli, R. A. A. Potential of chitin/chitosan-bearing materials for uranium recovery: an interdisciplinary review. *Carbohydr. Polym.* 84, 54–63 (2011).
18. Nilchi, A., Dehaghan, T. S. & Garmarody, S. R. Kinetics, isotherm, and thermodynamics for uranium and thorium ions adsorption from aqueous solutions by crystalline tin oxide nanoparticles. *Desalination* 321, 67–71 (2013).
19. Yusan, S. *et al.* Adsorption and thermodynamic behavior of U(VI) on Tendurek volcanic tuff. *J. Radioanal. Nucl. Chem.* 283, 231–238 (2010).
20. Fortin, C., Dutel, L. & Garnier-Laplace, J. Uranium complexation and uptake by a green alga in relation to chemical speciation: the importance of free uranyl ion. *Environ. Toxicol. Chem.* 23(4), 974–981 (2004).
21. Kazy, S. K., Souza, S. F. D. & Sar, P. Uranium and thorium sequestration by *Pseudomonas* sp.: mechanism and chemical characterization. *J. Hazard. Mater.* 163, 65–72 (2009).
22. Banato, M., Ragnasdottir, K. V. & Allen, G. F. Removal of uranium (VI), lead (II) at the surface of TiO₂ nanotubes studied by X-ray photoelectron spectroscopy, water air, and soil pollut. *Water Air Soil Pollut* 2012(223), 3845–3857 (2012).
23. Crane, R. A., Dickinson, M. & Scott, T. B. Nanoscale zero-valent iron nanoparticles for the remediation of plutonium and uranium contaminated solutions. *Chem. Eng. J.* 262, 319–325 (2015).
24. Noubactep, C., Caré, S. & Crane, R. Nanoscale metallic iron for environmental remediation: prospects and limitations. *Water Air Soil Pollut.* 223(3), 1363–1382 (2012).
25. Riba, O., Scott, T. B., Ragnasdottir, K. V. & Allen, G. C. Reaction mechanism of uranyl in the presence of zero-valent iron nanoparticles. *Geochim. Cosmochim. Acta* 72, 4047–4057 (2008).
26. Scott, T. B., Popescu, I. C., Crane, R. A. & Noubactep, C. Nano-scale metallic iron for the treatment of solutions containing multiple inorganic contaminants. *J. Hazard. Mater.* 186, 280–287 (2011).
27. Elwakeel, K. Z., Atia, A. A. & Guibal, E. Fast removal of uranium from aqueous solutions using tetraethylenepentamine modified magnetic chitosan resin. *Bioresour. Technol.* 160, 107–114 (2014).
28. Elwakeel, K. Z. & Atia, A. A. Uptake of U(VI) from aqueous media by magnetic Schiff's base chitosan composite. *J. Clean. Prod.* 70, 292–302 (2014).
29. Elwakeel, K. Z., Hamza, M. F. & Guibal, E. Effect of agitation mode (mechanical, ultrasound and microwave) on uranium sorption using amine- and dithione-functionalized magnetic chitosan hybrid materials. *Chem. Eng. J.* 411, 128553 (2021).
30. Hamza, M. F. *et al.* Phosphorylation of guar gum/magnetite/chitosan nanocomposites for uranium (VI) sorption and antibacterial application. *Molecules* 26, 1920. <https://doi.org/10.3390/molecule26071920> (2021).
31. Hamza, M. F. *et al.* U(VI) and Th(IV) recovery using silica beads functionalized with urea- or thiourea-based polymers: application to ore leachate. *Sci. Total Environ.* 821, 153184 (2022).
32. Doyle, F. M. Ion flotation-its potential for hydrometallurgical operations. *Int. J. Min. Proc.* 72, 387–399 (2003).
33. Matis, K. A. & Mavros, P. Recovery of metals by ion flotation from dilute aqueous solutions. *Sep. Pur. Rev.* 20(1), 1–48 (1991).
34. Zouboulis, A. I. & Matis, K. A. Ion flotation in environmental technology. *Chemosphere* 16(2–3), 623–631 (1987).
35. Walkowiak, W., Maciejewski, P., Ulewicz, M., Kozłowski, C. Ion flotation with macrocyclic compounds: a review, XIX-Th ARS SEPARATORIA—Złoty Potok, Poland, 58–65 (2004)
36. Shakir, K., Benyamin, K. & Aziz, M. Separation of U(VI) from aqueous solutions by precipitate flotation with 8-quinolinol and surfactants. *Can. J. Chem.* 62, 51–55 (1984).
37. Lazaridis, N. K., Hourzemanoglou, A. & Matis, K. A. Flotation of metal-loaded clay anion exchangers. Part II: the case of arsenates. *Chemosphere* 47(3), 319–324 (2002).
38. Matis, K. A., Zouboulis, A. I. & Lazaridis, N. K. Heavy metals removal by biosorption and flotation. *Water Air Soil Pollut.: Focus* 3, 143–151 (2003).
39. Matis, K. A., Zouboulis, A. I., Lazaridis, N. K. & Hancock, I. C. Sorptive flotation for metal ions recovery. *Int. J. Min. Proc.* 70(1–4), 99–108 (2003).
40. Matis, K. A., Zouboulis, A. I., Gallios, G. P., Erwe, T. & Blöcher, C. Application of flotation for the separation of metal-loaded zeolites. *Chemosphere* 55(1), 65–72 (2004).
41. Rubio, J. & Tessele, F. Removal of heavy metal ions by adsorptive particulate flotation. *Min. Eng.* 10(7), 671–679 (1997).
42. Gao, P., Chen, X., Shen, F. & Chen, G. Removal of chromium (VI) from wastewater by combined electrocoagulation–electroflotation without a filter. *Sep. Purif. Technol.* 43, 117–123 (2005).
43. Obushenko, T. I., Astrelin, I. M., Tolstopalova, N. M., Varbanets, M. A. & Kondratenko, T. A. Wastewater treatment from toxic metals by floater extraction. *J. Water. Chem. Technol.* 30(4), 241–245 (2008).
44. Perlova, O. V. & Shirlova, A. A. Uranium (VI) floater extraction isolation from dilute aqueous solutions with electrolyte additions presence (in Russian). *Odessa Natl Univ. Herald* 15(13), 86–96 (2010).
45. Mamoukaris, A., Mimis, S., Karakolios, E., Xipolitos, K. & Atsioura, G. P. New friendly to environment method in wastewater treatment. *J. Environ. Prot. Ecol.* 15(3), 1021–1027 (2014).
46. Miranda, R. *et al.* The efficiency of chitosans for the treatment of papermaking process water by dissolved air flotation. *Chem. Eng. J.* 231, 304–313 (2013).
47. Palaniandy, P., Adlan, M. N., Aziz, H. A. & Murshed, M. F. Application of dissolved air flotation (DAF) in semi-aerobic leachate treatment. *Chem. Eng. J.* 157(2–3), 316–322 (2010).
48. Stoica, L., Constantin, C. & Lacatusu, I. Collector reagents for heavy metal ions separation from polluted aqueous systems. *J. Environ. Prot. Ecol.* 13(2), 486–496 (2012).

49. Stoica, L. and Constantin C. Depollution of aqueous systems, Good practice handbook (Depoluarea sistemelor apoase, Ghid de buna practică) (in Romanian), vol.1, Politehnica Press Publishing House, Bucharest, Romania (2010)
50. Stoica, L., Jitaru, I., Georgescu, D., Filip, D., Razvan, A., Petrescu, S. Molybdenum recovery from aqueous residual solutions in uranium ores processing in Proc. Uranium Mining and Hydrogeology, Freiberg, Germania, ISBN 3-87361-267-4, 319–330 (1998)
51. Stoica, L. Ionic and molecular flotation, Theory, methods and applications (Flotația ionică și moleculară Bazele teoretice, metode și aplicații), (in Romanian), Editura Didactică și Pedagogică Publishing House, Bucharest, Romania (1997)
52. Stoica, L., Catuneanu, R. & Filip, Gh. Decontamination of solutions containing radioactive substances by dissolved air flotation. *Water. Res.* **29**(9), 2108–2112 (1995).
53. Krestou, A. and Pnias, D. Uranium (VI) speciation diagrams in the $\text{UO}_2^{2+}/\text{CO}_3^{2-}/\text{H}_2\text{O}$ system at 25°C The European Journal of Mineral Processing and Environmental Protection Vol. 4, No. 2, 1303–0868, pp. 113–129 (2004)
54. Hashim, M. A., Mukhopadhyay, S., Sahu, J. N. & Sengupta, B. Remediation technologies for heavy metal contaminated groundwater. *J. Environ. Manag.* **92**, 2355–2388 (2011).
55. WHO, 1989. Evaluation of certain food additives and contaminants, Thirty-third Report of the Joint FAO/WHO Expert Committee on Food Additives, World Health Organisation Technical Report Series 776, Geneva, 1989, ISBN 92 4 120776 0, ISSN 0512-3054, 25
56. Popescu (Hostuc), I.C., Stoica, L., Constantin, C. & Stanescu, A.M. Equilibrium and kinetics of U(VI)aq adsorption on *in situ* generated $\text{Fe}_2\text{O}_3 \cdot n\text{H}_2\text{O}$. *Rev. de Chimie*, **70**(10), 3482–3485 (2019)
57. Waite, T. D., Davis, J. A., Payne, T. E., Waychunas, G. A. & Xu, N. Uranium (VI) adsorption to ferrihydrite: application of a surface complexation model. *Geochim. Cosmochim. Acta* **58**, 5465–5478 (1994).
58. Argun, M. E., Dursun, S., Ozdemir, C. & Karatas, M. Heavy metal adsorption by modified oak sawdust. Thermodynamics and kinetics. *J. Hazard. Mater.* **141**, 77–85 (2007).
59. Hsi, C.K.-D. & Langmuir, D. Adsorption of uranyl onto ferric oxyhydroxides: application of the surface complexation site-biding model. *Geochemica et Cosmochimica Acta* **49**, 1931–1941 (1985).
60. Stoica, L., and Constantin, C. 2010. Depollution of aqueous media. Good practice guide (Depoluarea sistemelor apoase. Ghid de buna practica), In Romanian vol.1, 2010, Politehnica Press, Bucharest
61. IUPAC Solubility Data Project: Solubility Data Series, International Union of Pure and Applied Chemistry, Pergamon Press, Oxford, (1979–1992)
62. Scott, T.B., Popescu, I.C., Crane, R.A., Noubactep, C. Nano-scale metallic iron for the treatment of solutions containing multiple inorganic contaminants, *J Hazard Mater.* **186**(1), 280–287 doi:<https://doi.org/10.1016/j.jhazmat.2010.10.113> (2011)
63. Kulkarni, R. D. & Somasundaran, P. Flotation chemistry of hematite/oleate system. *Colloids Surf.* **1**, 387–405 (1980).
64. Wang, N., Hsu, C., Zhu, L., Tseng, S., Hsu, J.-P. Influence of metal oxide nanoparticles concentration on their zeta potential, *J.C.I.S.*, **407**, 22–28 (2013)
65. Lahann, R. W., 1976. Surface charge variation in aging ferric hydroxide, *Clays and Clay Minerals*, **24**, 320–326. Pergamon Press 1976. Printed in Great Britain.
66. Heinänen, J., Jokela, P. & Ala-Peijari, T. Use of dissolved air flotation in potable water treatment in Finland. *Water Sci. Technol.* **31**(3–4), 225–238 (1995).
67. WHO Uranium in Drinking-water Background document for development of WHO Guidelines for Drinking-water Quality (2012)
68. Leja, I. 1982. Surface chemistry of froth flotation, Plenum, New York.
69. Wazne, M., Korfiatis, G. P. & Meng, X. Carbonate effects on hexavalent uranium adsorption by iron oxyhydroxide. *Environ. Sci. Technol.* **37**, 3619–3624 (2003).
70. Boyd, C.E., 2015. Chapter 3 Review of basic chemistry, solubility and chemical equilibrium in Water quality: An introduction, 2nd Edition, Springer International Publishing, Switzerland.
71. Cornelis, R., Caruso, J., Crews, H., Heumann, K. 2005. Chapter 5 Actinides elements in Handbook of elemental species II-Species in the Environment, food, medicine and occupational health, Wiley, England, UK, 521–534.
72. Dean, J. A. Section 8 Electrolytes, electromotive force and chemical equilibrium in Lange's handbook of chemistry, 15th Edition printed by McGraw-Hill Inc. USA, 841–856 (1999)
73. Cissoko, N., Zhang, Z., Zhang, J. & Xu, X. Removal of Cr (VI) from simulative contaminated groundwater by iron metal. *Process Saf. Environ. Prot.* **87**, 395–400 (2009).
74. Aoki, T. & Munemori, M. Recovery of chromium (VI) from wastewaters with iron (III) hydroxide-I Adsorption mechanism of chromium (VI) on iron (III) hydroxide. *Water Res.* **16**, 793–796 (1982).
75. Mitchell, P.C.H. Speciation of molybdenum compounds in water Ultraviolet spectra and REACH read across Report for the International Molybdenum Association REACH Molybdenum Consortium, 1–28 (2009)
76. Sena, M. M., Scarminio, I. S., Collins, K. E. & Collins, C. H. Speciation of aqueous chromium (VI) solutions with the aid of Q-mode factor analysis followed by oblique projection. *Talanta* **53**, 453–461 (2000).
77. Saric, A., Music, S. & Nomura, K. Influence of urotropine on iron oxides from FeCl_3 solutions. *Croat. Chem. Acta* **71**(4), 1019–1038 (1998).
78. Avram, M., Mateescu, Gh. D. Infra-Red Spectrometry. Applications in Organic Chemistry ("Spectroscopia în Infraroșu. Aplicații în Chimia Organică") in Romanian, Ed. Tehnica, București (1966)
79. Fedoseev, A.M. et al. Interaction of Pu(IV,VI) Hydroxides/Oxides with Metal Hydroxides/Oxides in Alkaline Media. Report No. PNNL-11900, Pacific Northwest National Laboratory, Richland, WA (1998)
80. Saputra, A. H., Qadhaiya, L. & Pitaloka, A. B. Synthesis and characterization of carboxymethyl cellulose (CMC) from water hyacinth using ethanol-isobutyl alcohol mixture as the solvents. *Int. J. Chem. Eng. Appl.* **5**(1), 36–40 (2014).
81. Singh, R., Misra, V. & Singh, R. P. Synthesis, characterization, and role of zero-valent iron nanoparticle in removal of hexavalent chromium from chromium—spiked soil. *J. Nanopart. Res.* **13**, 4063–4073 (2011).
82. Wang, J. & Somasundaran, P. Adsorption and conformation of carboxymethyl cellulose at solid-liquid interfaces using spectroscopic, AFM and allied techniques. *J. Colloid Interface Sci.* **291**, 75–83 (2005).
83. Andrade, A. L. et al. Synthesis and characterization of magnetic nanoparticles coated with silica through a sol-gel approach. *Ceramica* **55**, 420–424 (2009).
84. Nakamoto, K. (2009). Infrared and Raman Spectra of Inorganic and Coordination Compounds, 6th Edition, Wiley, New Jersey.
85. Niculescu, M. et al. Thermal and spectroscopic studies of Ni(II) - Fe(III) heteropolynuclear coordination compound obtained through the reaction of 1,2-ethanediol with metallic nitrates. *Rev. Roum. Chim.* **58**(6), 543–552 (2013).
86. Krehula, S. & Music, S. Influence of ruthenium ions on precipitation of α - FeOOH , α - Fe_2O_3 , and Fe_3O_4 in highly alkaline media. *J. Alloys Compd.* **416**, 284–290 (2006).
87. Keith, L.S., Faroon, O. M. and Fowler, B. A., 2015. Chapter 49 Uranium in: Handbook on the Toxicology of Metals 4th Edition, Elsevier.
88. Madhavi, V., Prasad, T. N. V. K. V. & Madhavi, G. Synthesis and spectral characterization of iron based micro and nanoparticles. *Iran. J. Energy Environ.* **4**(4), 385–390 (2013).

Acknowledgements

We would like to acknowledge the University “Politehnica” of Bucharest, Faculty of Applied Chemistry and Materials Science, Department of Inorganic Chemistry, Physical-Chemistry and Electrochemistry, and R&D National Institute for Metals and Radioactive Resources (INCDMRR-ICPMRR, Bucharest, Romania) staff for the support in conducting this work. We would also like to thank Prof. Dr. Thomas B. Scott and Dr. Richard A. Crane from the Interface Analysis Centre of the University of Bristol for the Fe-based nanomaterials provided. We would also like to express our gratitude for the reviewers’ hard work, helping us with extremely inspiring recommendations, constructive and objective criticism, pertinent questions, and remarks. Therefore, the dialogue was very dynamic and fruitful, creating a friendly atmosphere for making the best science.

Author contributions

C.C., L.S., and I.-C. P. wrote the main manuscript text and prepared the figures. O.O. performed TG–DTA analysis. All the authors reviewed the manuscript.

Competing interests

The authors declare no competing interests.

Additional information

Correspondence and requests for materials should be addressed to I.-C.P.

Reprints and permissions information is available at www.nature.com/reprints.

Publisher’s note Springer Nature remains neutral with regard to jurisdictional claims in published maps and institutional affiliations.



Open Access This article is licensed under a Creative Commons Attribution 4.0 International License, which permits use, sharing, adaptation, distribution and reproduction in any medium or format, as long as you give appropriate credit to the original author(s) and the source, provide a link to the Creative Commons licence, and indicate if changes were made. The images or other third party material in this article are included in the article’s Creative Commons licence, unless indicated otherwise in a credit line to the material. If material is not included in the article’s Creative Commons licence and your intended use is not permitted by statutory regulation or exceeds the permitted use, you will need to obtain permission directly from the copyright holder. To view a copy of this licence, visit <http://creativecommons.org/licenses/by/4.0/>.

© The Author(s) 2022